2014

Development of Flat Tube Heat Exchanger for Heat Pump Air Conditoner

Takuya Matsuda
Living Environment Systems Laboratory, Mitsubishi Electric Corporation, matutaku2020cosmoplt@gmail.com

Akira Ishibashi
Living Environment Systems Laboratory, Mitsubishi Electric Corporation, Ishibashi.Akira@ab.MitsubishiElectric.co.jp

Takashi Okazaki
Living Environment Systems Laboratory, Mitsubishi Electric Corporation, Okazaki.Takashi@eb.MitsubishiElectric.co.jp

Keisuke Hokazono
Air-Conditioning & Refrigeration Systems Works, Mitsubishi Electric Corporation,
Hokazono.Keisuke@bp.MitsubishiElectric.co.jp

Daisuke Shimamoto
Air-Conditioning & Refrigeration Systems Works, Mitsubishi Electric Corporation,
Shimamoto.Daisuke@db.MitsubishiElectric.co.jp

See next page for additional authors

Authors
Takuya Matsuda, Akira Ishibashi, Takashi Okazaki, Keisuke Hokazono, Daisuke Shimamoto, and Hiroki Okazawa

Development of Flat Tube Heat Exchanger for Heat Pump Air Conditioner

Takuya MATSUDA[1]*, Akira ISHIBASHI[1], Takashi OKAZAKI[1], Keisuke HOKAZONO[2], Daisuke SHIMAMOTO[2], Hiroki OKAZAWA[2]

[1]Living Environmental Systems Laboratory, Mitsubishi Electric Corporation, Shizuoka-city, Shizuoka, Japan
Phone: +81-54-287-3053, E-mail: matutaku2020cosmoplt@gmail.com

[2]Air-Conditioning $ Refrigeration Systems Works, Mitsubishi Electric Corporation, Wakayama-city, Wakayama, Japan

ABSTRACT

We developed a new type of an aluminum flat tube heat exchanger for a heat pump outdoor unit in order to improve the energy efficiency of the heat pump system. When applying flat tube heat exchangers to heat pump outdoor units, it is difficult to achieve good condensation coil drainage, high performance during frost accumulation, and even refrigerant distribution. In order to achieve the same condensation coil drainage and performance during frost accumulation as conventional round tube heat exchangers, the flat tubes were inserted in newly designed plate fins with ellipse cutouts. In order to achieve the even distribution of refrigerant, an aluminum distributor and 3-way pipes were installed leading to the evaporator.
First we describe features of the flat tube heat exchanger. Next, we present and explain experimental effects of the air-side heat transfer coefficient and the air-side pressure drop for dry, wet, and frost coil conditions. Moreover, we present experimental results of the total heat transfer performance when the flat tube heat exchanger is treated as an evaporator and when it is treated as a condenser. Finally, we explain the overall heat transfer performance of the flat tube heat exchanger and compare it to a conventional circular tube heat exchanger in the case that the each are utilized in a heat pump outdoor unit.

1. INTRODUCTION

In recent years, energy regulations have become stricter in light of global warming. Accordingly, air conditioner and heat pump manufacturers have improved the energy efficiency of their products by improving the performance of the products' compressors, heat exchangers, fans, etc, and through advancements in refrigerant cycle control technology.
We have developed a heat exchanger with enhanced performance by optimizing the fin pattern and using a smaller tube. A study about an air conditioner development that reduced the weight by being equipped with a flat tube heat exchanger which could increase the air side heat transfer through brazing and decrease the air side pressure drop was reported. However, when applying the flat tube heat exchanger to heat pump outdoor units, it is difficult to achieve good condensation coil drainage, high performance even with frost accumulation, as well as even refrigerant distribution. Also, it is difficult to apply a flat tube heat exchanger to an air conditioner or heat pump of a large capacity because it requires many rows of tubes in the heat exchanger.
In this paper, we examine the specifications of flat tube heat exchanger which can be mounted into a large capacity air conditioner.

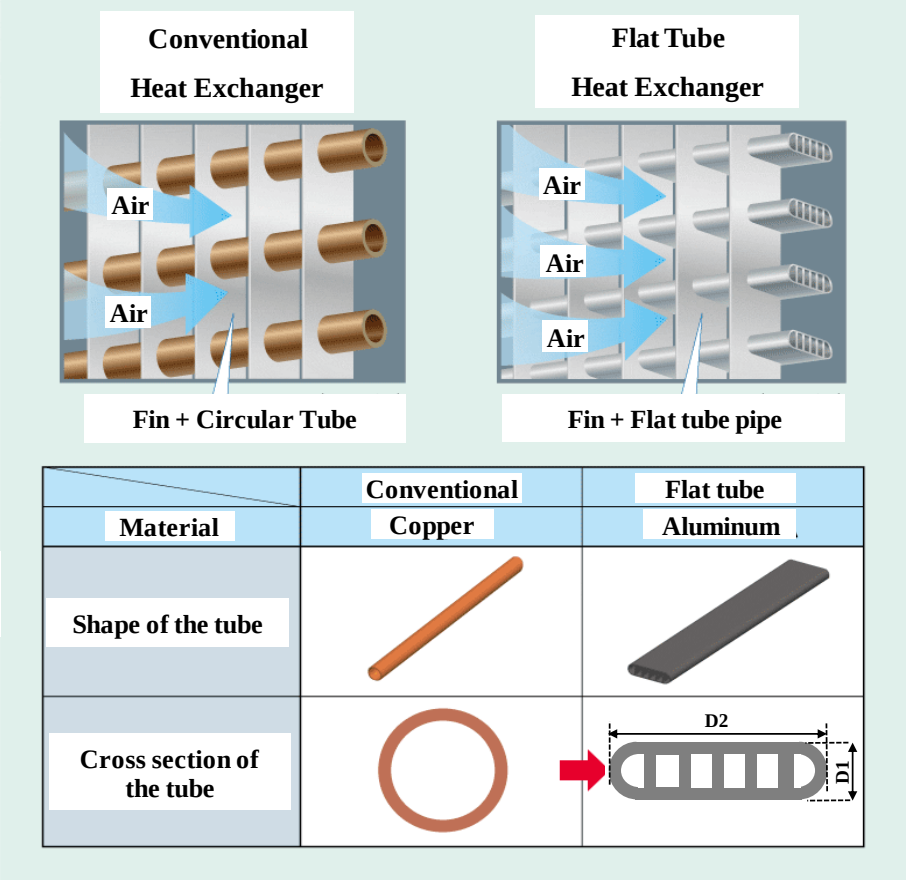

Fig.1 Flat tube heat exchanger for air conditioner

2. Short Length D1 of Flat Tube

First of all, we examined the effect of the short length D1 of the flat tube on the overall heat transfer A_oK, the air side pressure drop ΔP_{air}, and the number of paths was analyzed for a 10HP outdoor unit.
The overall heat resistance $1/A_oK$ of the heat exchanger is defined by the equation (1). A_o is the overall surface area of the heat exchanger, K is the overall heat transfer coefficient, α_o is the air side heat transfer coefficient, A_i is the inner surface area of the tube, α_i is the refrigerant side heat transfer coefficient in the tube.

$$\frac{1}{A_o K} = \frac{1}{A_o \alpha_o} + \frac{1}{A_i \alpha_i} \tag{1}$$

Fig.2 shows the calculation results of the relationship between the overall heat transfer A_oK of the flat tube heat exchanger and the air side pressure drop ΔP_{air} of the heat exchanger when the short length D1 of the flat tube is 2 mm, 4 mm, and 6 mm (the long length D2 is 15 mm). It was assumed that the refrigerant side pressure loss was the same for all flat tubes of different short lengths. The calculation results of the conventional heat exchanger with the 7.94 mm diameter circular tube are shown in Fig.2. The air side heat transfer coefficient α_o and the pressure drop ΔP_{air} were calculated by CFD (Computational Fluid Dynamics). The refrigerant side heat transfer coefficient α_i and the pressure drop ΔP_{ref} were calculated by an empirical formula (Koyama, 2002). In the calculation, the row pitch was 17.7 mm and the step pitch was set so that the unit performance was the maximum. The analysis shows that the overall heat transfer A_oK of the flat tube heat exchanger becomes larger as the short length D1 becomes smaller. It

also shows that the overall heat transfer A_oK of the flat tube heat exchanger is larger than that of a conventional heat exchanger when the ΔP_{air} of the flat tube heat exchanger is same as the ΔP_{air} of the conventional heat exchanger.
Fig.3 shows the relationship between "path number" and "step number" when the heat exchanger is mounted in a heat pump outdoor unit. It is assumed that the refrigerant side pressure loss is the same for the flat tube design and the circular tube design. According to the Fig.3, the path number increases as the short length D1 decreases.
Design parameters for the development of the flat tube heat exchanger include: hair-pin type flat tube, 3 or more rows of pipes, and a "counter-flow type" path pattern when the heat exchanger is used as a condenser (Fig.4). In order to use three rows of tubes, the hair-pin tube design, and the "counter-flow type" path pattern, a "step number/path number" ratio of more than 2 is required. Based on the calculation results, we chose the short length D1 of 4 mm for testing because it had the largest A_oK values.

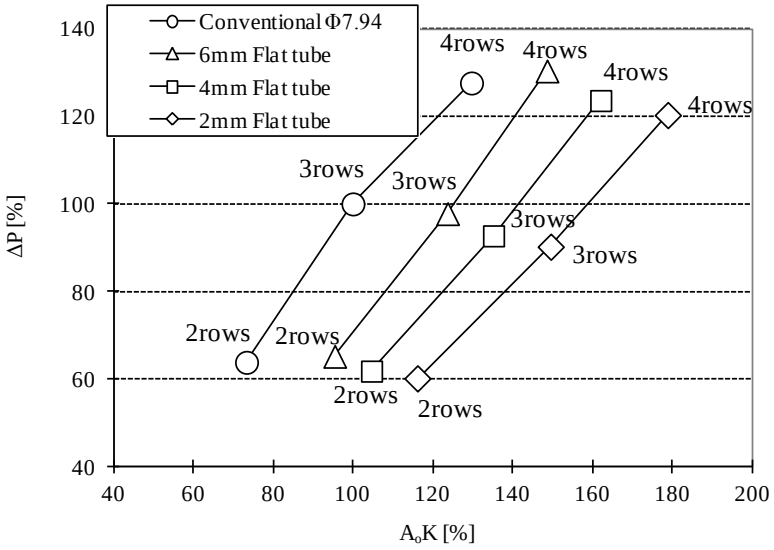

Fig. 2 Relationship between A_oK and ΔP

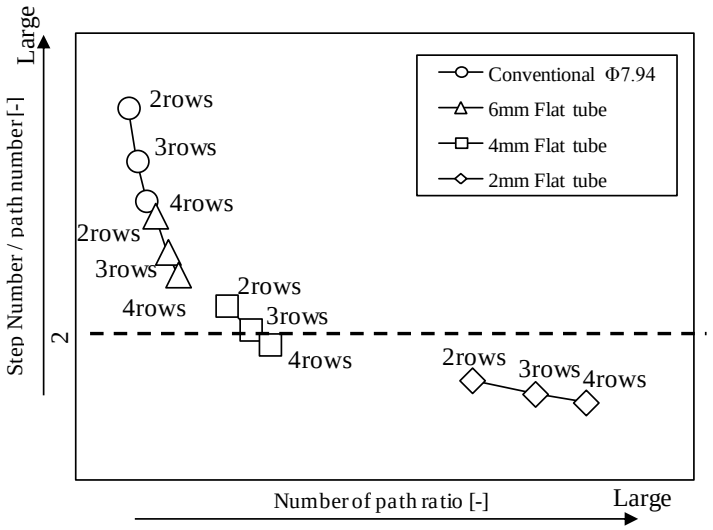

Fig.3 Step number divided by path number

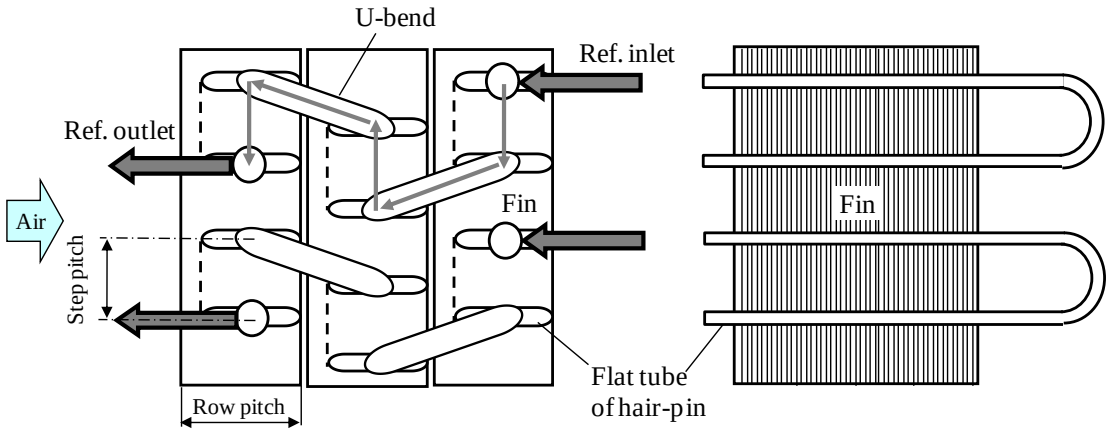

Fig.4 Path pattern of "counter-flow type" and Hair-pin tube

3. Air Side Performance Measurement

3.1 Experimental Apparatus

Fig.5 shows the schematic view of the experimental apparatus. Test heat exchangers are put into the wind tunnel and the wind tunnel is in a constant temperature and humidity room. The wind tunnel has a square cross section with dimensions of 300 x 300 mm. A honeycomb flow straightener, a thermocouple grid, a dew point meter, pressure taps, a test heat exchanger, and a fan are installed in the wind tunnel. The fluid flowing in the test heat exchanger pipe is water or brine. The fluid temperature is measured by the sheathed resistance thermometer (Pt100, ClassA). The mass flow rate of the fluid is measured by the coriolis mass flow meter (Accuracy: ±0.2%, R.D.). The airside temperature is measured by the thermocouple grid (Accuracy: ±0.1°C). The dew-point temperature is measured by the mirror surface cooling type dew-point meter (Accuracy: ±0.2°C). The air flow rate is measured by the ultrasonic volume flow meter (Accuracy: ±0.03%, F.S.). The pressure drop is measured by the differential pressure meter (Accuracy: ±0.1Pa).

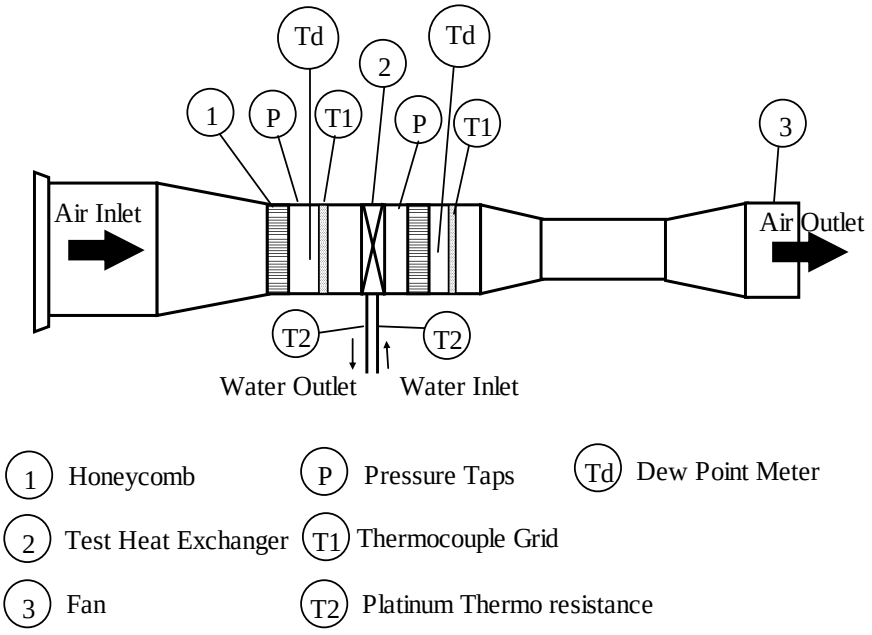

Fig.5 Experimental apparatus

3.2 Test Heat Exchanger

Table 1 shows the specifications of the test heat exchangers. The tube diameter of the conventional heat exchanger is 7.94 mm and the external dimensions of the flat tube are 4 x 15mm. The channel number of the flat tube is 6. The fin coating of the conventional heat exchanger is either non-hydrophilic coating or a hydrophilic coating. The fin coating of the flat tube heat exchanger is a non-hydrophilic coating. The fin shape of the conventional heat exchanger is *cross-stair slit*. The fins of the flat tube heat exchanger are newly designed plate fins with ellipse cutouts. The flat tubes are inserted in the ellipse cutouts and the connecting part of the plate fins is arranged to the windward side. During the operation under the frost condition, the temperature of the front tip part of the fin can rise and can prevent the frost accumulation of the front tip. Furthermore, condensation can drain down the connecting part of the fin.

Table1. Specifications of Test Heat Exchanger

	Conventional heat exchanger	**Flat tube heat exchanger**
Tube diameter [mm]	7.94	4 x 15
Number of channels [-]	1	6
Step pitch [mm]	20.4	15.3
Row pitch [mm]	17.7	17.7
Number of rows [-]	2	2
Number of path number [-]	2	6
Fin pitch [mm]	1.6	1.6
Step number [-]	14	18
Fin height [mm]	285.6	275.4
Surface treatment	Hydrophilic or Non-Hydrophilic coating	Non-Hydrophilic coating
Fin pattern	Cross stair slit 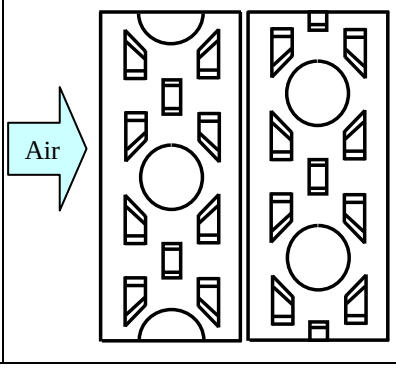	3-slit 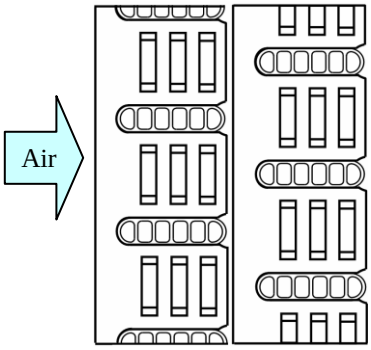

3.3 Experimental Conditions and Method

Table 2 shows the experimental conditions. The air side heat transfer coefficient α_o and the pressure drop ΔP_{air} are measured for 3 different fin conditions; dry, wet, and frost surface. For the dry surface condition, the inlet temperature of air is 20°C, the fluid in the tube is water, and the inlet temperature of the water is 50°C. The air side heat transfer coefficient α_o is calculated by using the formula of Dittus-Boelter and the calculated water side heat transfer coefficient α_i and the measured overall heat transfer coefficient K.

For the wet surface condition, the inlet air temperature is 27°C, the inlet air absolute humidity of 10.5 g/kg, the fluid in the tube is water, and the inlet water temperature is 10°C.

For the frost surface condition, the inlet air temperature is 2°C, the inlet air absolute humidity is 3.7 g/kg, the air velocity is 1.5 m/s, the fluid in the tube is brine, the inlet temperature of the brine is -5 °C, and the brine flow rate is 6 liters/min.

Table 2 Experimental Conditions

Surface Condition of Fin	Dry	Wet	Frost
Inlet Temperature of Air [°C]	20	27	2
Inlet Absolute Humidity of Air [g/kg]	-	10.5	3.7
Air Velocity [m/s]	1, 1.5, 2	1, 1.5, 2	1.5
Fluid	Water	Water	Brine
Flow Rate [liters/min]	18-24	18-24	6
Inlet Temperature of Fluid [°C]	50	10	-5

3.4 Experimental Results

3.4.1 Dry surface condition

Fig.6, 7 shows the experimental results of the air side heat transfer coefficient α_o and the pressure drop ΔP_{air} to the air velocity for the dry surface condition. When the air velocity is 1.5m/s, the air side heat transfer coefficient α_o of the flat tube heat exchanger is 15% larger than that of the conventional heat exchanger. The α_o of the flat tube heat exchanger is higher than that of the conventional heat exchanger because of higher fin efficiency due to the lower contact resistance at the brazed connections between the fins and the pipe.

When the air velocity is 1.5m/s, the air side pressure drop ΔP_{air} of the flat tube heat exchanger is 9% smaller than that of the conventional heat exchanger. This is because the minimum passing cross section of the flat tube heat exchanger is larger than that of the conventional flat tube heat exchanger.

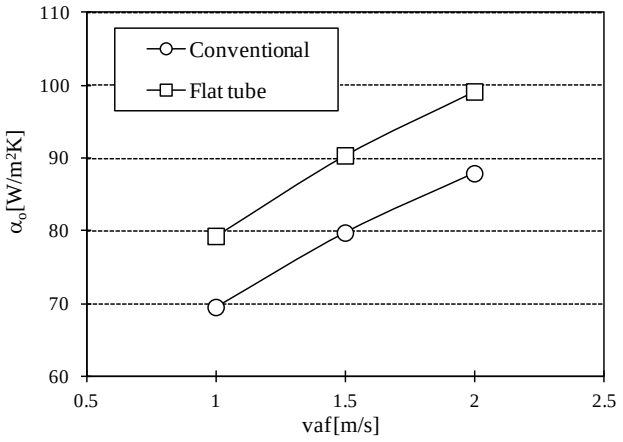

Fig. 6 Air Side Heat Transfer Coefficient α_o
(On dry surface condition)

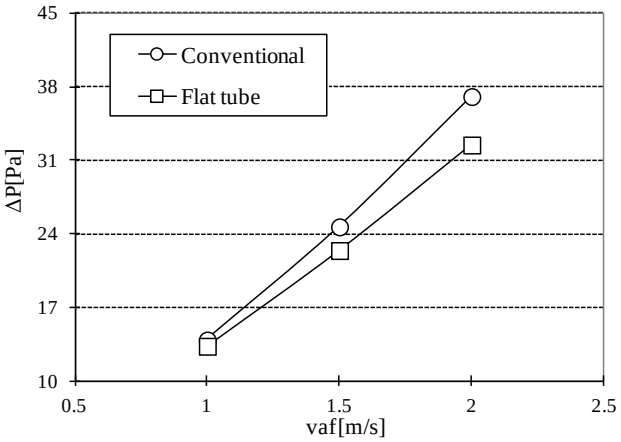

Fig. 7 Air Side Pressure Drop ΔP
(On dry surface condition)

3.4.2 Wet Surface Condition

The ratio of the pressure drop of the wet surface condition to that of the dry surface condition $\Delta P_{wet}/\Delta P_{dry}$ is defined as the drainage performance. Fig.8 shows the relationship between the wind speeds and the increasing ratio of the pressure drop $\Delta P_{wet}/\Delta P_{dry}$ to the air velocity. $\Delta P_{wet}/\Delta P_{dry}$ of the conventional heat exchanger with non-hydrophilic fins becomes larger as the air velocity increases. However, the $\Delta P_{wet}/\Delta P_{dry}$ ratio of the conventional heat exchanger with hydrophilic fins and the flat tube heat exchanger are relatively steady as the air velocity increases. Moreover, $\Delta P_{wet}/\Delta P_{dry}$ of the flat pipe heat exchanger is smaller than the conventional heat exchanger with none-hydrophilic fins, and equivalent to the conventional heat exchanger with hydrophilic fins. The reason why $\Delta P_{wet}/\Delta P_{dry}$ of the conventional heat exchanger with non-hydrophilic fins becomes larger as the air velocity increases is because the dew condensation water is held between the fins as the air velocity increases; the water droplet contact angle on the

fins is large. In the case of the flat tube heat exchanger, the water droplet contact angle is smaller due to brazing, and the amount of the water held between the fins can be smaller.

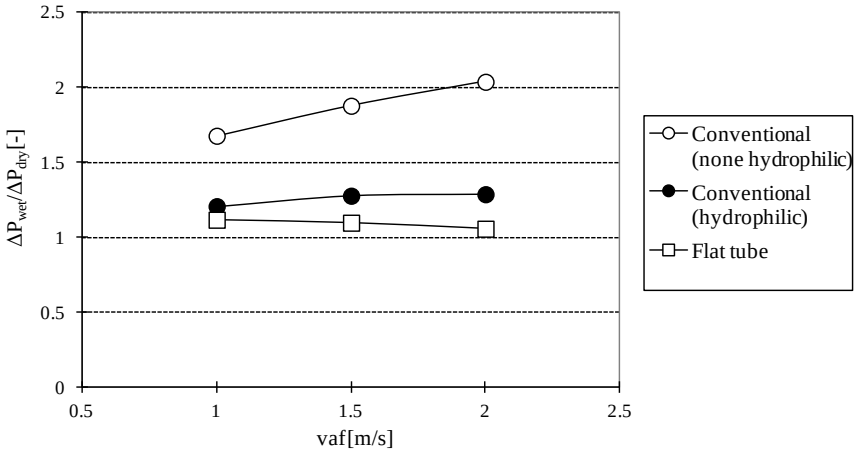

Fig.8 Increasing Ratio of $\Delta P_{wet}/\Delta P_{dry}$

3.4.3 Frost Surface Condition

Fig.9 shows the air side pressure drop ΔP_{air} plotted against the the mass of frost accumulation. The frost weight change ΔM is given by formula (2). Ga is the air mass flow rate and (Xa1 – Xa2) is the absolute humidity difference between the inlet and the outlet. The total amount of frost weight M is calculated by formula (3). Here 'n' is time at which the air side pressure drop ΔP_{air} reaches 150Pa.

With the same mass of frost, the air side pressure drop ΔP_{air} of the flat tube heat exchanger is smaller than that of the conventional heat exchanger. Since the minimum passing cross section of the flat tube heat exchanger is larger than that of the conventional heat exchanger, the flat tube heat exchanger will have more space for the bypass air flow even if the frost grows around the flat tube.

$$\Delta M = G_a \cdot \left(X_{a1} - X_{a2}\right) \cdot \Delta t \tag{2}$$

$$M = \sum_{i=1}^{n} \Delta M \tag{3}$$

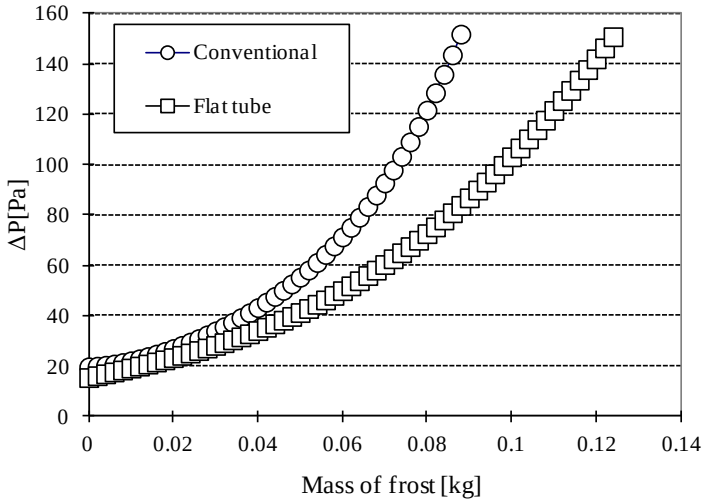

Fig.9 Air Side Pressure Drop ΔP
(On frost surface condition)

4. Refrigerant Distribution Measurement Results

The refrigerant distributor is a combination of a multi-branched distributer and 3-way pipes as seen in figure Fig.10. This experiment using water-air was carried out to measure the refrigerant distribution.

4.1 Experimental Apparatus and Conditions

Fig.11 and Table 3 shows the experimental apparatus and the experimental conditions. The two-phase flow pattern of water-air was correlated to the flow pattern of R410A by using the modified Baker chart (1983, Hashizume). The experimental conditions have two cases: case1 (Gr=125 kg/h, x=0.2) and case2 (Gr=200kg/h, x=0.2).

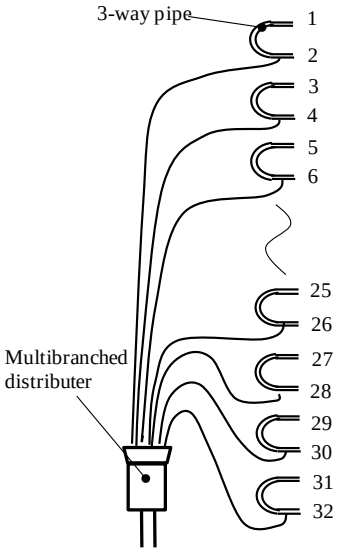

Fig.10 Configuration of Refrigerant Distributer

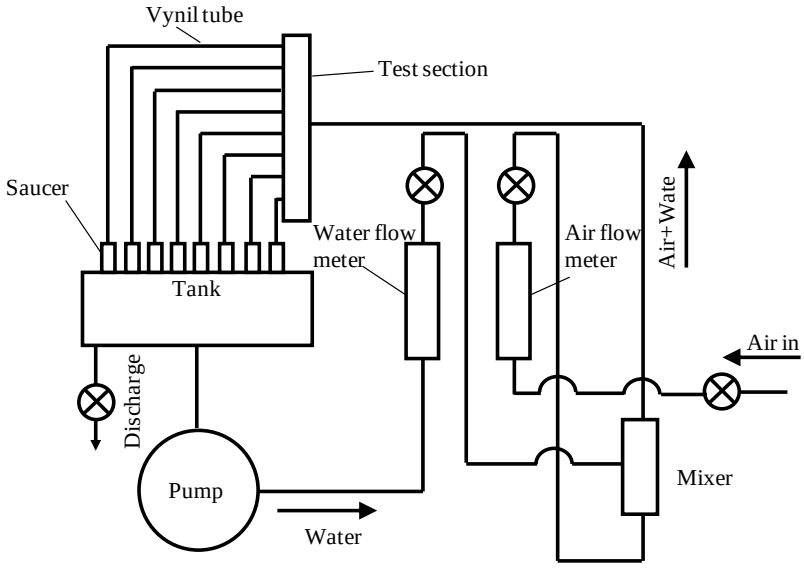

Fig.11 Experimental Apparatus

Table 3 Experimental conditions

	R410A (Target)		**Water – Air**	
	Mass flow rate: Gr [kg/h]	Quality: x [-]	Water flow rate [l/min]	Air flow rate [l/min]
Case 1	125	0.2	1.48	56
Case 2	200	0.2	2.36	89.6

4.2 Experimental Results

Fig.12 shows the mass flow ratio of water for each branch. The two-phase flow of water-air is distributed into the coil via the multi-branched distributor, and through the 3-way pipes. The coefficient of variation (the ratio between the standard deviation and the mean value) of the water distribution ratio data is 7%, and not influenced by changing the mass flow rate. The reason why the coefficient of variation is low is because the flow through of the multi-branched distributer is relatively uniform. Furthermore, water-air which passes the multi-branched distributer is dispersed evenly by the collision with the horizontal pipe wall of the 3-way pipe, which allows the liquid film to form evenly inside of the pipe.

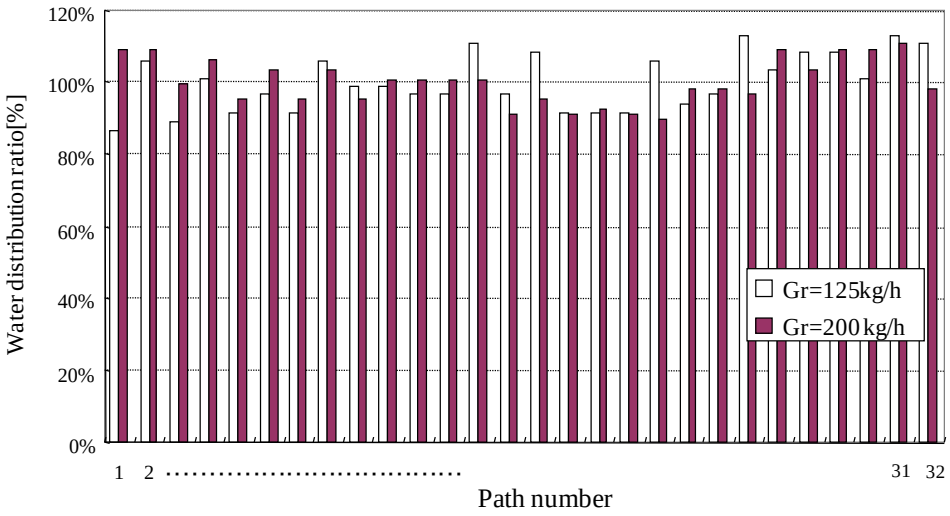

Fig.12 Refrigerant Distribution Characteristic

5. Measurement of Overall Heat Transfer Performance A_oK

5.1 Specification of Heat Exchanger

The flat tube heat exchanger and the conventional heat exchanger was mounted into the 10HP outdoor unit respectively, and then the over heat transfer A_oK was evaluated from the capacity. The air side temperature (inlet & outlet) and the temperature of the refrigerant were measured. Table 4 shows the specifications of the test heat exchanger mounted into the outdoor unit.

Table 4 Specifications of Heat Exchanger

	Conventional heat exchanger	**Flat tube heat exchanger**
Row number [-]	2.5	2.33
Height [mm]	1224	1224
Width [mm]	1770	1770
Path number [-]	14	32

5.2 Experimental Results

Fig.13 shows the experimental results of the overall heat transfer performance A_oK. The vertical axis shows the ratio of the heat transfer performances of the flat tube heat exchanger and the conventional heat exchanger. The calculated A_oK, which is found from the experimental result of the air side heat transfer coefficient α_o and the refrigerant side heat transfer coefficient α_l, is shown in the same figure. The refrigerant side heat transfer coefficient α_i is calculated by the experimental formula (Koyama, 2002). The calculated condensing A_oK of the flat tube heat exchanger was 32% larger than that of the conventional heat exchanger and the evaporating A_oK of the flat tube heat exchanger was 36% larger. The deviation between the calculation and the experimental results of the overall heat transfer performance A_oK was within 3%.

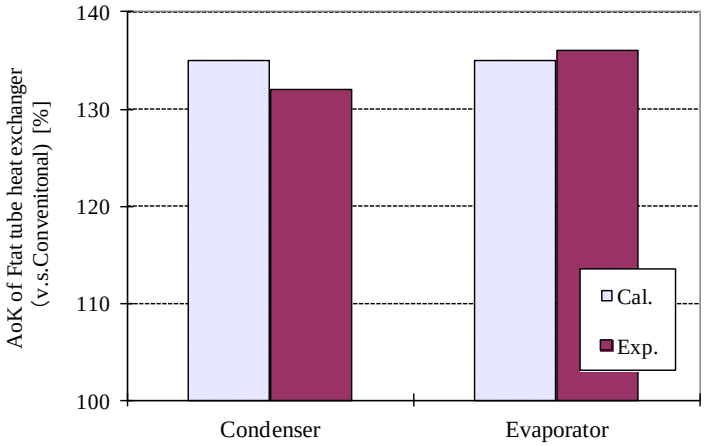

Fig.13 Overall Heat Transfer Performance A_oK

6. Conclusions

We developed a new type of an aluminum flat tube heat exchanger for the heat pump outdoor unit. We presented and explained experimental results of the air-side heat transfer coefficient and the air-side pressure drop for dry, wet, and frost conditions. Moreover, we presented the refrigerant distribution in 32 branches when using the flat tube heat exchanger. Finally, we presented the overall heat transfer AoK of the flat tube heat exchanger which was mounted into the 10HP outdoor unit. Conclusions are as follows:

- The air side heat transfer coefficient α_o of the flat tube heat exchanger was 15% larger and the ΔP of the flat tube heat exchanger was 9% smaller than those of the conventional heat exchanger for the dry condition.
- The ratio $\Delta P_{wet}/\Delta P_{dry}$ of the flat pipe heat exchanger was smaller than the conventional heat exchanger with non-hydrophilic fins, and equivalent to the conventional heat exchanger with hydrophilic fins.
- The air side pressure drop ΔP of the flat tube heat exchanger was smaller than that of the conventional heat exchanger for the frost condition.
- The coefficient of variation of the refrigerant distribution for the flat tube heat exchanger was 7% and was not influenced by changing the mass flow rate.
- The condensing A_oK of the flat tube heat exchanger was 32% larger than that of the conventional heat exchanger. The evaporating A_oK of the flat tube heat exchanger was 36% larger, which basically matched our hypothetical and expected outcome.

NOMENCLATURE

D1	short length of flat tube	(mm)
D2	long length of flat tub	(mm)
A_o	overall surface area	(mm^2)
A_i	refrigerant surface area	(mm^2)
α_o	air side heat transfer coefficient	(W/m^2K)
ΔP	air side pressure drop	(Pa)
α_i	refrigerant side heat transfer coefficient	(W/m^2K)
K	overall heat transfer coefficient	(W/m^2K)
X_{a1}	inlet absolute humidity of air	(kg/kg)
X_{a2}	outlet absolute humidity of air	(kg/kg)
Gr	refrigerant mass flow rate	(kg/hour)

REFERENCES

A. Ishibashi, et al., 2014, Development of the flat-tube heat exchanger for air conditioner, SHASE & JSRAE conference

T. Kamata, et al., 2012, Development of all aluminum micro channel heat exchanger for air conditioner, 2012 JSRAE Annual Conference, p.37-40

S. Koyama, et al., 2002, An experimental study on condensing heat transfer characteristics of pure refrigerant HFC134a in a multi-port extruded tube, trans. of the JSRAE, vol. 19-1

K. Hashizume, et al., 1983, Flow pattern and void fraction of refrigerant two-phase flow in a horizontal pipe, Trans. of the JSRAE(B), 49(437)

T. Matsuda, et al., 2010, Heat transfer and pressure drop characteristics of cross stair slit fin, 15th International Refrigeration and Air Conditioning Conference at Pudue, 2261

T. Matsuda, et al., 2010, Development of the indoor heat exchanger with small tubes for packaged air conditioners